

Reversible Plasmonic Circular Dichroism of Au Nanorod and DNA Assemblies

Zhengtao Li, Zhening Zhu, Wenjing Liu, Yunlong Zhou, Bing Han, Yan Gao, and Zhiyong Tang*

Laboratory for Nanomaterials, National Center for Nanoscience and Technology, No. 11 Beiyitiao, Zhongguancun, Beijing 100190, China

Supporting Information

ABSTRACT: Reversible plasmonic circular dichroism (CD) responses are realized for the first time based on temperature-dependent assembly and disassembly of Au nanorod (Au NR) and DNA hybrids. Compared with the conventional UV–vis absorption spectra, the changes in both intensity and line shape of plasmonic CD signals are much more pronounced, leading to a preliminary detection limit of DNA as low as 75 nM. The mechanism and influence factors of reversible plasmonic CD responses are explored.

The plasmonic circular dichroism (CD) responses of the hybrid nanostructures containing noble metal nanoparticles (NPs) and chiral molecules have received increasing research interest at the frontier of both nanophotonics and conventional spectroscopy,¹ stemming from various applications in chemistry, biology, and optics of these novel metamaterials.² The plasmonic CD responses are generally believed to originate from the chiral current inside noble metal NPs, which is induced by the dipole of the attached chiral molecules including cysteine, peptide, DNA, and chiral fiber.^{1,3} Among the above chiral molecules, DNA is the most attractive one because its programmability provides an excellent platform for constructing the hybrids with noble metal NPs in a controllable way.^{4,5} Nevertheless, previous studies on the plasmonic CD responses have been mostly focused on their origin, transcription, and amplification,^{1,6–9} and there is no report on dynamic and reversible responses until now, though they are very important for future application. Herein, we fabricate the hybrid of Au nanorods (Au NRs) and DNA, and demonstrate that the dynamic assembly of DNA modified Au NRs gives rise to reversible change of plasmonic CD responses including the peak shape and intensity. Impressively, the reversible change of plasmonic CD responses could be used as a new detection method for ultrasensitive sensors.

Figure 1 illustrates the reversible plasmonic CD responses of Au NRs and DNA assemblies by changing the temperature. First of all, Au NRs (Figure S1a) with the mean aspect ratio of 3.0 are modified with single-strand (SS-) DNA (sequence A, blue curves in Figure 1, see Supporting Information (SI) for detailed sequence) due to strong interaction between Au and mercapto group of DNA.^{4,5} Subsequently, SS-DNA stabilized Au NRs are incubated with its cDNA (green curves in Figure 1, see SI for detailed sequence) containing the sticky end of four extra bases (red curve in figure 1) to form double-strand (DS-) DNA modified Au NRs. Such DS-DNA modified Au NRs remain separate in solution if the solution temperature (60 °C) is higher than its melting temperature (50 °C).^{4d} Since DNA is a chiral molecule with distinct CD signals at UV region (the maxima of the bisignated CD peaks are, respectively, located at 247 and 271 nm, Figure S2),^{3b} the coupling between surface plasmon resonances (SPR) of Au NRs and the chiral signal of DNA will induce generation of plasmonic CD at the visible region (red line in Figure 2a). As expected, there are two CD peaks appearing at 512 and 698 nm, corresponding to peak positions of transverse and longitudinal SPR of Au NRs, respectively.⁶ Because the sticky end of DS-DNA can further be complementary with each other when the temperature is cooled to 20 °C, spontaneous aggregation of Au NRs without the predominant structure occurs, which is confirmed by both scanning electron microscope (SEM) and dynamic light scattering (DLS) observations (Figures S3–S6). With the random aggregation, it is reasonable that the length of DNA is much shorter than that of Au NRs, so that DNA cannot

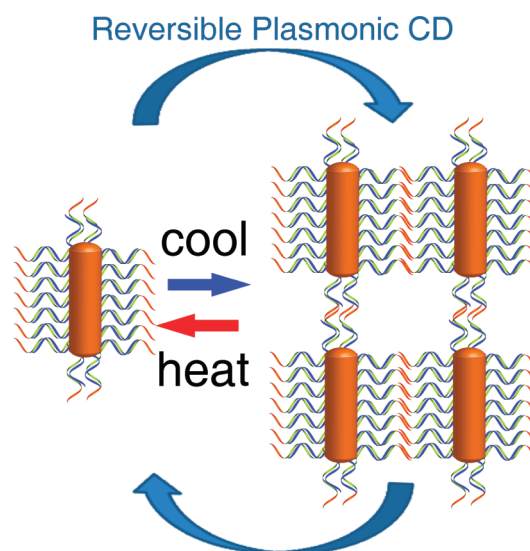


Figure 1. Scheme of reversible plasmonic CD responses based on dynamic assembly and disassembly of double-strand DNA modified Au NRs (yellow column) at different temperature. Au NRs are modified with single-strand DNA (blue curves) and its complementary DNA (green curves) with the sticky end (red curves).

DNA modified Au NRs. Such DS-DNA modified Au NRs remain separate in solution if the solution temperature (60 °C) is higher than its melting temperature (50 °C).^{4d} Since DNA is a chiral molecule with distinct CD signals at UV region (the maxima of the bisignated CD peaks are, respectively, located at 247 and 271 nm, Figure S2),^{3b} the coupling between surface plasmon resonances (SPR) of Au NRs and the chiral signal of DNA will induce generation of plasmonic CD at the visible region (red line in Figure 2a). As expected, there are two CD peaks appearing at 512 and 698 nm, corresponding to peak positions of transverse and longitudinal SPR of Au NRs, respectively.⁶ Because the sticky end of DS-DNA can further be complementary with each other when the temperature is cooled to 20 °C, spontaneous aggregation of Au NRs without the predominant structure occurs, which is confirmed by both scanning electron microscope (SEM) and dynamic light scattering (DLS) observations (Figures S3–S6). With the random aggregation, it is reasonable that the length of DNA is much shorter than that of Au NRs, so that DNA cannot

Received: November 2, 2011

Published: February 7, 2012

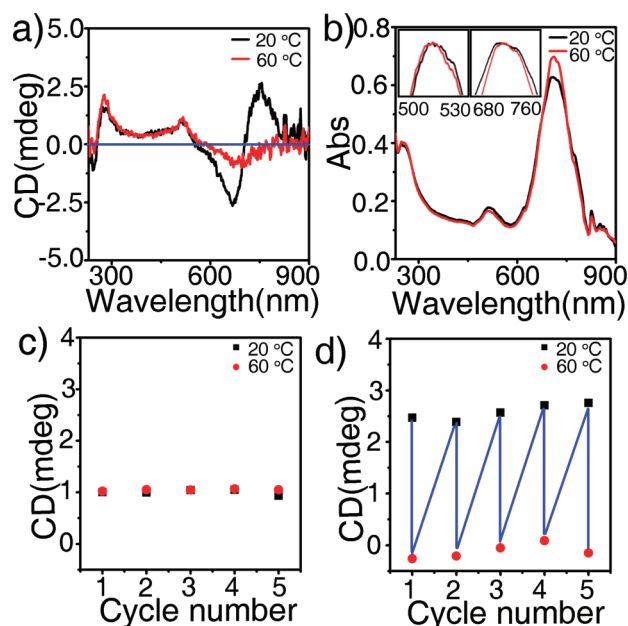


Figure 2. Reversible plasmonic CD (a) and corresponding UV-vis absorption spectra (b) of DNA modified Au NRs at 20 °C (black line) and 60 °C (red line). Au NRs with mean aspect ratio 3.0 are modified with single-strand DNA (sequence A) and its complementary DNA with the sticky end. The insets are the enlarged UV spectra. CD intensity at 512 nm (c) and 750 nm (d) cycled at 20 °C (black dots) and 60 °C (red dots). The concentrations of Au NRs and the complementary DNA with the sticky end are 0.18 nM and 75 nM, respectively.

become the chiral template for three-dimensional (3D) arrangement of Au NRs. These results also reveal that the mechanism of chiral placement of nanoparticles in 3D geometry is not the key factor for generation of plasmonic CD in our system. The black curve in Figure 2a shows a significant change in plasmonic CD response after Au NRs aggregate. The longitudinal plasmonic CD peak separates into two bands at 750 and 670 nm with the opposite sign and remarkably increased intensity, while the transverse one keeps almost unaltered. The bisignated line shape for the CD spectrum stands for the coupling of chiral signal of DNA with longitudinal SPR of Au NRs at both symmetric (antibonding π^* -peak) and antisymmetric (bonding π -peak) hybrid modes (Figure S7).¹⁰ The reason behind different changes in the longitudinal and transverse plasmonic CD responses is that the hotspot enhancement happens mainly at the end of Au NRs during aggregation, because SPR of Au NRs mostly distribute at their end parts.¹¹ Therefore, the transverse peak is not sensitive to aggregation of Au NRs as compared to its longitudinal counterpart, and the similar result is found in the corresponding UV-vis absorption spectra (Figure 2b). Nevertheless, different changes in plasmonic CD responses at different wavelength regions will benefit the target detection; for example, the insensitive CD signal at 512 nm can be used as an internal standard. It should be noted that both the symmetric line shape of the longitudinal plasmonic CD and the unchanged transverse plasmonic CD sign indicate that the retardation effect and the coupling between the longitudinal and transverse modes during Au NR aggregation may not be very strong.⁸ Furthermore, the same change trend in plasmonic CD responses is universal for DNA with different length and sequence (Figures S8, S9).

As comparison, Figure 2b shows the UV-vis absorption spectra of DS-DNA modified Au NRs and their assembly at varying temperature. When the temperature is decreased from 60 to 20 °C, the transverse peak in UV-vis spectrum is red-shifted from 511 to 516 nm with slightly increased intensity, and meanwhile, the longitudinal peak becomes broad with reduced intensity (Figure 2b and the insets). Evidently, the change in UV-vis absorption features is much smaller than that in plasmonic CD responses with respect to both the line shape and intensity of the peaks. One of the most convincing causes is that in addition to electronic transitions (these are the basis for UV-vis absorption characterization), plasmonic CD responses are much more sensitive to the configuration transformation of nanostructures.¹² Therefore, plasmonic CD responses could be used as a substitute of conventional UV-vis absorption in the ultrasensitive sensors such as target DNA detection. Meanwhile, because the CD spectra are very sensitive to chiral molecules, the signal change of plasmonic CD could be used as a sensor for recognizing chiral molecules, which is very difficult to accomplish using UV-vis detection. As an example, the concentration of complementary DNA with the sticky end used in Figure 2b is 75 nM, which is comparable and even lower than that of classical UV-vis detection methods based on Au NP aggregation.^{4e} It is noteworthy that the above preliminary results are obtained without any optimization, and it can be expected that the detection limit will be further improved by controlling the experimental conditions such as the temperature of the solution (Figure S10) and salt concentration.

One of the important characteristics of DNA-based assembly is its reversibility. Since aggregation of Au NRs is based on the interaction between the sticky ends of DS-DNA, they will be presumed to separate from each other when the solution temperature is changed back to 60 °C. As a result, concomitant plasmonic CD should change reversibly with the temperature. The experimental results with five cycles between 20 and 60 °C confirm that the CD signal at 512 nm is almost unchanged (Figure 2c), while the CD signal at 750 nm switches between 2.5 and 0 stably (Figure 2d).

The plasmonic CD responses can be manipulated by altering the experimental parameters. First, different amount of complementary DNA with the sticky end is added to the solution containing SS-DNA modified Au NRs. When the amount of complementary DNA with the sticky end is increased (Figure 3a), the intensity of the longitudinal plasmonic CD peak is simultaneously enhanced. This is easily understood because increasing amount of complementary DNA with the sticky end induces large aggregation of Au NRs, which consolidates the coupling between DNA helix and Au NRs.⁶ Second, Au NRs with different aspect ratios are used for assembly. When the aspect ratios are reduced from 2.8 to 2.1 (Figure S1), the longitudinal plasmonic CD signals of Au NRs at the aggregate state show an obvious blue shift (Figure 3b). The zero-crossing points of the longitudinal plasmonic CD peaks are around 636, 652, and 675 nm for assemblies of Au NRs with aspect ratios 2.1, 2.4, and 2.8, respectively. The blue shift of plasmonic CD responses is reasonable considering that the longitudinal SPR peak of Au NRs with a small aspect ratio is located at the short wavelength. When the aspect ratio is 2.4, the intensity of the longitudinal plasmonic CD peaks is the strongest. This phenomenon originates from two counteractive effects: (1) As the aspect ratio of Au NRs increases, their longitudinal SPR signals are enhanced. (2) The coupling between longitudinal SPR of Au NRs and chiral signal of DNA

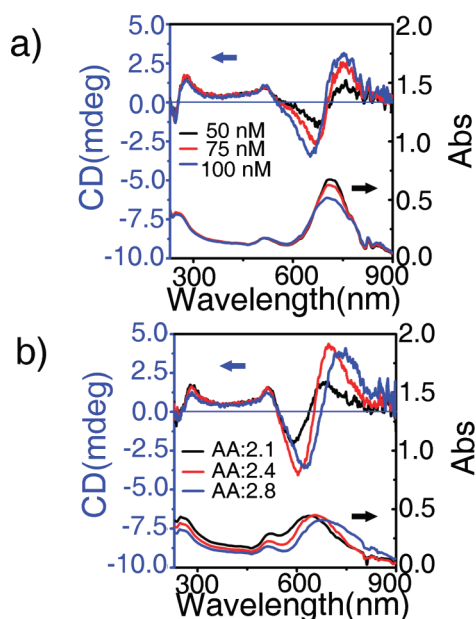


Figure 3. CD and corresponding UV-vis absorption spectra of Au NR assemblies at 20 °C with varying concentration of complementary DNA containing the sticky end (a) or varying aspect ratio of Au NRs (b). In panel a, black, red, and blue curves stand for 50, 75, and 100 nM complementary DNA with the sticky end in the solutions, respectively. The concentration of SS-DNA (sequence A) modified Au NRs with the aspect ratio of 3.0 is 0.18 nM. In panel b, black, blue, and red curves correspond to the DNA-based assemblies containing Au NRs with the aspect ratios (AA) of 2.1, 2.4, and 2.8, respectively. The concentrations of SS-DNA (sequence B) modified Au NRs with different aspect ratios are around 0.2 nM. The concentrations of its complementary DNA with the sticky end in the solutions of Au NRs are 75 nM.

is reduced as the difference in the wavelengths of the absorption peaks between DNA (260 nm) and Au NRs (630–687 nm) becomes large.⁶

Finally, To prove that the change in plasmonic CD responses at different temperature originates from the coupling between DNA and Au NRs, a series of control experiments are carried out. First, when complementary DNA without the sticky end is added to the solution of SS-DNA stabilized Au NRs, CD spectra remain unchanged with the temperature (Figure S11). This is because without the sticky end, DS-DNA modified Au NRs cannot spontaneously aggregate at 20 °C and Au NRs keep isolated in solution regardless of the temperature changes. Second, all the assembly conditions to obtain reversible plasmonic CD responses are the same, except that spherical Au NPs with the mean diameters of 18 and 35 nm are used as the substitutes of Au NRs. Interestingly, there are no obvious temperature-dependent CD responses appearing during assembly and disassembly of DS-DNA modified Au NPs (Figures S12–S14). It is understood that the plasmonic coupling of Au NPs is much weaker than that between Au NRs,^{1d} and thus, the change in plasmonic CD responses at varying temperature is also not so evident. This result highlights the crucial role that the anisotropic shape of Au nanocrystals play in generation of strong plasmonic CD signals and the corresponding temperature-dependent change.

In conclusion, we have demonstrated that the hybrids of DNA and Au NRs produce remarkable plasmonic CD signals at the visible light region. With the help of complementary DNA

with the sticky end, the plasmonic CD responses could be tuned reversibly at different temperature. As the DNA-guided NP assembly has been broadly used for constructing complex structures and for detecting target molecules, the plasmonic CD responses obtained by the DNA and Au NRs hybrids will shed light on creating intelligent materials with unique optical responses as well as fabricating ultrasensitive sensors.

■ ASSOCIATED CONTENT

● Supporting Information

Detailed experimental methods, DNA sequences, TEM, SEM, DLS, and CD spectra. This material is available free of charge via the Internet at <http://pubs.acs.org>.

■ AUTHOR INFORMATION

Corresponding Author

zytang@nanoctr.cn

Notes

The authors declare no competing financial interest.

■ ACKNOWLEDGMENTS

This work was supported financially by the National Natural Science Foundation for Distinguished Youth Scholars of China (21025310, Z.T.), National Natural Science Foundation of China (21003026, Y.G.; 20973047 and 91027011, Z.T.), National Research Fund for Fundamental Key Project (2009CB930401, Z.T.), and 100-Talent Program of Chinese Academy of Sciences (Z.T.).

■ REFERENCES

- (1) (a) George, J.; Thomas, K. G. *J. Am. Chem. Soc.* **2010**, *132*, 2502–2503. (b) Qi, H.; Shopsowitz, K. E.; Hamad, W. Y.; MacLachlan, M. J. *J. Am. Chem. Soc.* **2011**, *133*, 3728–3731. (c) Molotsky, T.; Tali, T.; Ben, M. A.; Markovich, G.; Kotlyar, A. B. *J. Phys. Chem. C* **2010**, *114*, 15951–15954. (d) Guerrero-Martinez, A.; Auguie, B.; Alonso-Gomez, J. L.; Dzolic, D.; Gomez-Grana, S.; Zinic, M.; Cid, M. M.; Liz-Marzan, L. M. *Angew. Chem., Int. Ed.* **2011**, *50*, 5499–5503. (e) Gautier, C.; Burgi, T. *ChemPhysChem* **2009**, *10*, 483–492. (f) Lieberman, I.; Shemer, G.; Fried, T.; Kosower, E.; Markovich, G. *Angew. Chem., Int. Ed.* **2008**, *47*, 4855–4857.
- (2) (a) Xia, Y.; Zhou, Y.; Tang, Z. *Nanoscale* **2011**, *3*, 1374–1382. (b) Govan, J. E.; Jan, E.; Querejeta, A.; Kotov, N. A.; Gun'ko, Y. K. *Chem. Commun.* **2010**, *46*, 6072–6074. (c) Moloney, M. P.; Gun'ko, Y. K.; Kelly, J. M. *Chem. Commun.* **2007**, *38*, 3900–3902. (d) Berova, N.; Bari, L. D.; Pescitelli, G. *Chem. Soc. Rev.* **2007**, *36*, 914–931. (e) Pendry, J. B. *Science* **2004**, *306*, 1353–1355. (f) Gubler, U.; Bosshard, C. *Nat. Nanotechnol.* **2002**, *1*, 209–210. (g) Gao, Y.; Tang, Z. Y. *Small* **2011**, *7*, 2133–2146. (h) Aherne, D.; Gara, M.; Kelly, J. M.; Gun'ko, Y. K. *Adv. Funct. Mater.* **2010**, *20*, 1329–1338.
- (3) (a) Shukla, N.; Bartel, M. A.; Gellman, A. J. *J. Am. Chem. Soc.* **2010**, *132*, 8580–8575. (b) Shemer, G.; Kruchevski, O.; Markovich, G.; Molotsky, T.; Lubitz, I.; Kotlyar, A. B. *J. Am. Chem. Soc.* **2006**, *128*, 11006–11007. (c) Chen, W.; Bian, A.; Agarwal, A.; Liu, L.; Shen, H.; Wang, L.; Xu, C.; Kotov, N. A. *Nano Lett.* **2009**, *9*, 2153–2159. (d) Zhou, Y.; Zhu, Z.; Huang, W.; Liu, W.; Wu, S. J.; Liu, X.; Gao, Y.; Zhang, W.; Tang, Z. *Angew. Chem., Int. Ed.* **2011**, *50*, 11456–11459. (e) Li, Y.; Zhou, Y.; Wang, H.; Perrett, S.; Zhao, Y.; Tang, Z.; Nie, G. J. *Angew. Chem., Int. Ed.* **2011**, *50*, 5860–5864. (f) Zhou, Y.; Yang, M.; Sun, K.; Tang, Z.; Kotov, N. A. *J. Am. Chem. Soc.* **2010**, *132*, 6006–6013.
- (4) (a) Loweth, C. J.; Caldwell, W. B.; Peng, X.; Alivisatos, A. P.; Schultz, P. G. *Angew. Chem., Int. Ed.* **1999**, *38*, 1808–1812. (b) Sharama, J.; Chhabra, R.; Andersen, C. S.; Gothelf, K. V.; Yan, H.; Liu, Y. *J. Am. Chem. Soc.* **2008**, *130*, 7820–7821. (c) Sharma, J.; Chhabra, R.; Cheng, A.; Brownell, J.; Liu, Y.; Yan, H. *Science* **2009**,

- 323, 112–116. (d) Jones, M. R.; Macfarlane, R. J.; Lee, B.; Zhang, J.; Young, K. L.; Senesi, A. J.; Mirkin, C. A. *Nat. Mater.* **2010**, *9*, 913–917.
- (e) Storhoff, J. J.; Elghanian, R.; Mucic, R. C.; Mirkin, C. A.; Letsinger, R. L. *J. Am. Chem. Soc.* **1998**, *120*, 1959–1964.
- (5) (a) Nykypanchuk, D.; Maye, M. M.; Lelie, D. V.; Gang, O. *Nature* **2008**, *451*, 549–552. (b) Li, Z.; Cheng, E.; Huang, W.; Zhang, T.; Yang, Z.; Liu, D.; Tang, Z. *J. Am. Chem. Soc.* **2011**, *133*, 15284–15287. (c) Cheng, W.; Campolongo, M. J.; Cha, J. J.; Tan, S. J.; Umbach, C. C.; Muller, D. A.; Luo, D. *Nat. Mater.* **2009**, *8*, 519–525. (d) Tan, S. J.; Campolongo, M. J.; Luo, D.; Cheng, W. *Nat. Nanotechnol.* **2011**, *6*, 268–276. (e) Akbulut, O.; Jung, J.; Bennett, R. D.; Hu, Y.; Jung, H.; Cohen, R. E.; Mayes, A. M.; Stellacci, F. *Nano Lett.* **2007**, *7*, 3493–3498. (f) Macfarlane, R. J.; Lee, B.; Jones, M. R.; Harris, N.; Schatz, G. C.; Mirkin, C. A. *Science* **2011**, *334*, 204–208.
- (6) Govorov, A. O.; Fan, Z.; Hernandez, P.; Slocik, J. M.; Naik, R. R. *Nano Lett.* **2010**, *10*, 1374–1382.
- (7) Govorov, A. O.; Bryant, G. W.; Zhang, W.; Skeini, T.; Lee, J.; Kotov, N. A.; Slocik, J. M.; Naik, R. R. *Nano Lett.* **2006**, *6*, 984–994.
- (8) Auguie, B.; Alonso-Gomez, J. L.; Guerrero-Martinez, A.; Liz-Marzan, L. M. *J. Phys. Chem. Lett.* **2011**, *2*, 846–851.
- (9) Guerrero-Martinez, A.; Alonso-Gomez, J. L.; Auguie, B.; Cid, M. M.; Liz-Marzan, L. M. *Nano Today* **2011**, *6*, 381–400.
- (10) Jain, P. K.; Eustis, S.; El-Sayed, M. A. *J. Phys. Chem. B* **2006**, *110*, 18243–18253.
- (11) Shao, L.; Woo, K. C.; Chen, H.; Jin, Z.; Wang, J.; Lin, H. Q. *ACS Nano* **2010**, *4*, 3053–3062.
- (12) Berova, N.; Nakanishi, K.; Woody, R. W. *Circular Dichroism: Principles and Applications*, 2nd ed.; Wiley-VCH: New York, 2000.